DIELECTRON PRODUCTION IN $p + p$ AND Au + Au COLLISIONS AT $\sqrt{s_{NN}} = 200$ FROM STAR*

Bingchu Huang

for the STAR Collaboration

University of Science and Technology of China, Hefei, 230026, China
and
Brookhaven National Laboratory, Upton, NY, 11973, USA

The dielectron spectra in the mass range $0 < M_{ee} < 3.3$ GeV/c^2 are measured at midrapidity ($|y| < 1$) by the STAR experiment in $p + p$ and Au + Au collisions at $\sqrt{s_{NN}} = 200$ GeV. The measured dilepton continuum is compared to hadronic cocktail simulations. The vector meson in-medium modification in the low mass region and the first result of dielectron elliptic flow are also presented. In addition, the ω yields via dileptonic decays are measured for $p + p$ and Au + Au collisions.

1. Introduction

Dilepton production is a crucial probe of strongly interacting matter since leptons can penetrate the hot and dense nuclear matter with little or no interactions. As such, leptons can probe the whole time evolution and dynamics of the heavy ion collisions. In-medium properties of vector mesons can be studied via their dileptonic decays in the low mass region (LMR: $M_{ll} < 1.1$ GeV/c^2). The observation of in-medium modifications of vector mesons may be related to the possibility of chiral symmetry restoration [1,2]. In the intermediate mass range (IMR: $1.1 < M_{ll} < 3.0$ GeV/c^2), dilepton will have a contribution from thermal radiation of the quark-gluon plasma (QGP) [1, 2], however $c\bar{c}$ production also contributes significantly [7]. The dilepton production could help to understand the properties of QGP and dynamic of heavy ion collisions.

---

* Presented at the Conference "Strangeness in Quark Matter 2011", Kraków, Poland, September 18–24, 2011.

The recent installation of full Time-of-Flight detector (TOF) at STAR significantly improved the electron identification (eID), especially in the low momentum region. In this paper, we present the STAR results on dielectron production in $p + p$ and $Au + Au$ collisions at $\sqrt{s_{NN}} = 200$. The first measurement on dielectron elliptic flow is also reported for 200 GeV $Au + Au$ collisions.

2. Data analysis

In this analysis, we have used two detectors for the eID: the Time Projection Chamber (TPC) and the Time-of-Flight Detector (TOF). The TPC is the primary tracking device of the STAR detector providing energy-loss, momentum and path-length measurements of particles created in the collisions. The ionization energy loss (dE/dx) is used for particle identification [3, 4]. In the year 2009, 72% of the TOF system was installed and operational. The TOF installation has been completed since, and extends the identification of π and K up to 1.6 GeV/c and the $p(\bar{p})$ up to 3 GeV/c [5, 6]. Each track included in the dielectron analysis was required to pass cuts of the velocity(β) from the TOF and the dE/dx from the TPC. Electrons can be clearly identified from low to intermediate p_{T} by combining the information from TOF and TPC in both $p + p$ and $Au + Au$ collisions. The electron purity in $p + p$ analysis is $\sim 99\%$ and $\sim 97\%$ in minimum-bias $Au + Au$ analysis by applying velocity and p_{T} dependent dE/dx cuts on tracks with $p_{\mathrm{T}} > 0.2$ GeV/c and $|\eta| < 1$.

The data sets include 107 million minimum bias $p + p$ events taken in year 2009, 220 million minimum bias, and 150 million central $Au + Au$ events taken in year 2010. The dielectron invariant mass distribution was generated by pairing all possible e^+ and e^- tracks from the same event, which is marked as unlike-sign distribution. In order to understand the combinatorial and correlated background, we reconstructed the backgrounds by both mixed-event and like-sign techniques. The invariant mass distributions for unlike-sign, like-sign, and mixed-event. In the like-sign technique, the invariant mass was calculated by pairing two tracks with same charge from the same events. The mixed-event background was reconstructed by two opposite charge sign electrons from different events. In the $M_{ll} < 0.7$ GeV/c^2 region, due to correlated background, from $e.g.$ cross pair and jet contribution [7], we subtracted acceptance corrected like-sign background. In the $M_{ll} > 0.7$ GeV/c^2 region, we subtracted normalized mixed event background since the mixed-event offers better statistics.

The dielectron elliptic flow v_2 is calculated by standard event plane method [8, 9, 10]. The signal v_2 can be calculated as:

$$v_2^{\text{Tot}}(m) = v_2^{\text{Sig}}(m)\frac{r(m)}{1 + r(m)} + v_2^{\text{Bg}}(m)\frac{1}{1 + r(m)} \,, \tag{1}$$

where $v_2^{\text{Tot}}(m)$ is the flow of the total candidates as a function of invariant mass, $v_2^{\text{Sig}}(m)$ and $v_2^{\text{Bg}}(m)$ is the flow of signal and background, respectively. The $r(m)$ is the signal-to-background ratio shown in Fig. 1. The v_2^{Sig} can be extracted by fitting the data of the v_2^{Tot} distributions to the Eq. (1).
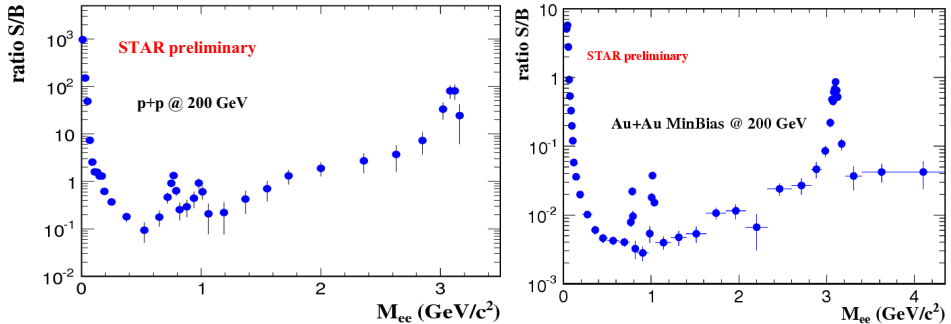
Fig. 1. The signal-to-background ratio in minimum-bias $p + p$ collisions (left) and minimum-bias $Au + Au$ collisions (right).

3. Results

The signal-to-background ratio in 200 GeV $p + p$ and $Au + Au$ collisions are shown in Fig. 1. Figure 2 (left panel) shows the efficiency corrected invariant mass spectrum within STAR acceptance from non-singly diffractive (NSD) $p + p$ collisions ($\sigma_{\text{NSD}} = 30.0 \pm 3.5$ mb [11]) compared to hadronic cocktail simulation. They are consistent with each other within error bars, and provide a base line for $Au + Au$ collisions. The details of the cocktail simulation procedure can be found in [12].

The measured $\omega \rightarrow e^+ e^-$ spectra in NSD $p + p$ and minimum-bias $Au + Au$ (0–80%) collisions are shown in Fig. 2 (right panel). The spectrum in $p + p$ collision is consistent with the previous measurement [14] and Tsallis Blast-Wave (TBW) fit [15] to high p_{T} (> 2 GeV/c) ω spectra [16]. The extrapolation of TBW fit from high to low p_{T} is consistent with the ω measurement at low p_{T}. In $Au + Au$ collisions, the ω p_{T} spectrum is consistent with TBW model prediction based on the fit to other hadrons [15]. The χ^2/ndf of the TBW prediction from light hadrons to ω spectra is 3/5. The average flow velocity of TBW fit parameter for the hadrons is 0.47 ± 0.01. This indicates that the ω meson has the same flow velocity as other light hadrons at freeze-out in $Au + Au$ collisions at $\sqrt{s_{NN}} = 200$ GeV.
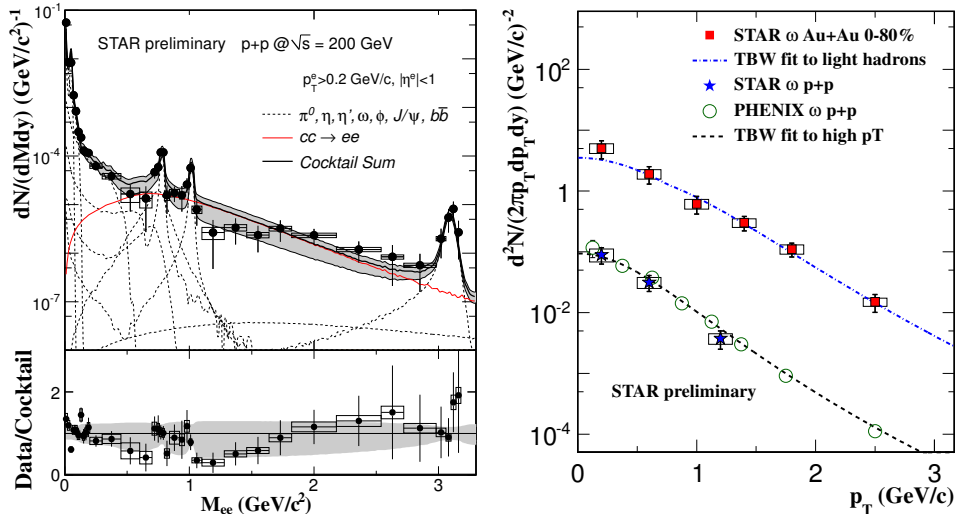
Fig. 2. Left: The comparison for dielectron continuum between data and simulation within STAR acceptance ($|y_{e^+e^-}| < 1$, $|\eta_e| < 1$, and $p_T(e) > 0.2$ GeV/c) in 200 GeV minimum-bias $p + p$ collisions. The dielectron continuum from simulations with different source contributions are also shown. The grey band is systematic error on cocktail, and the box represents systematic error on data. Right: The ω p_T spectra from 200 GeV $p + p$ and Au + Au collisions.

Fig. 3 shows the efficiency corrected dielectron spectra within STAR acceptance in Au + Au minimum-bias (left) and central (0–10%) collisions (right) [13]. In the LMR, an enhancement with a factor of $1.72 \pm 0.10^{\text{stat}} \pm 0.50^{\text{sys}}$ compare to cocktail (without ρ) has been observed in central Au + Au collisions. For minimum-bias Au + Au collisions, the enhancement factor is $1.53 \pm 0.07^{\text{stat}} \pm 0.41^{\text{sys}}$ (without ρ). In the IMR, the comparison between minimum-bias and central collisions shows that the yield from binary-scaled charm contributions from PYTHIA is overshooting the data in central collisions. This is possibly due to the modification of charm production in central Au + Au collisions at $\sqrt{s_{NN}} = 200$ GeV.

The first measurement of dielectron elliptic flow v_2 from minimum-bias Au + Au collisions at $\sqrt{s_{NN}} = 200$ GeV is shown in Fig. 4. The left panel shows the v_2 as a function of invariant mass of dielectron with statistical errors. The right panel shows the dielectron v_2 in the mass range $M_{ee} < 0.14$ GeV/c^2 (dominated by π^0 decayed dielectrons) as a function of p_T. The v_2 is consistent with the simulation of pion decayed dielectron v_2. The input π v_2 are measured by STAR [17] and PHENIX [18].
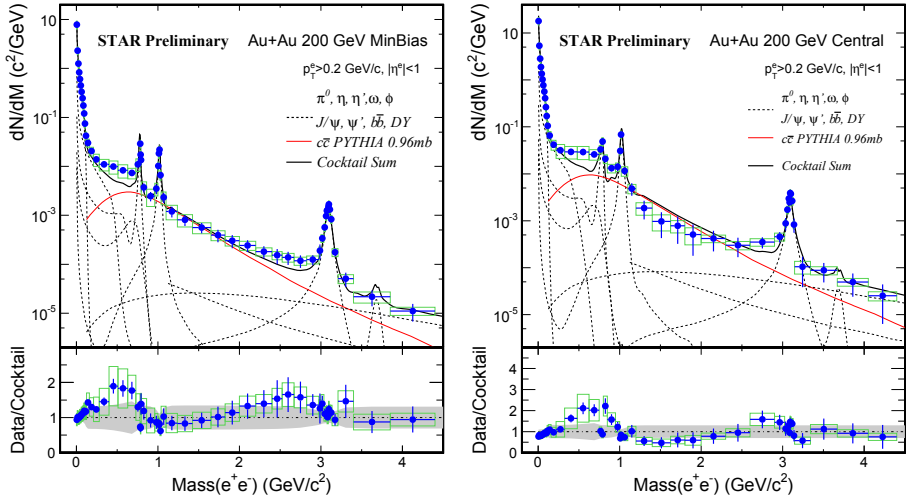
Fig. 3. Invariant mass spectra with the STAR acceptance from $\sqrt{s_{NN}} = 200$ GeV Au + Au minimum-bias (left) and top 10% central collisions (right). The grey band is systematic error on cocktail, and the box is systematic error on data.
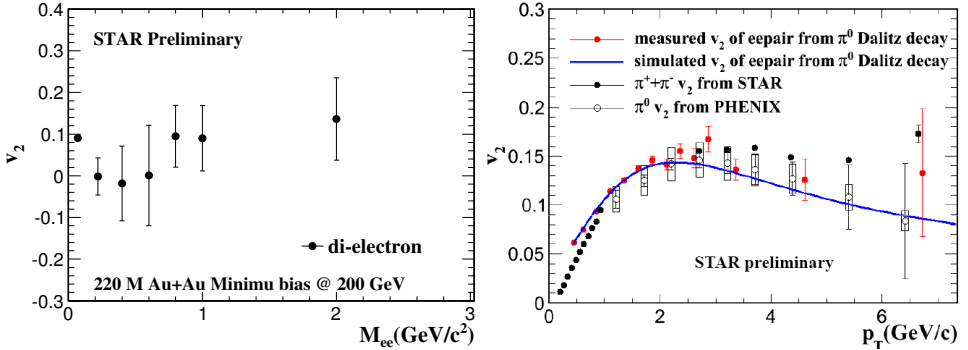
Fig. 4. Left: The dielectron elliptic flow v_2 as a function of invariant mass from minimum-bias Au + Au collisions at $\sqrt{s_{NN}} = 200$ GeV. Right: π^0 decayed dielectron v_2 as a function of p_T from minimum-bias Au + Au collisions at $\sqrt{s_{NN}} = 200$ GeV. Black points are STAR measured $\pi^+ + \pi^-$ v_2. Open circles are PHENIX measured π^0 v_2. The solid (blue) line represents the simulation of π decayed dielectron v_2.

4. Summary

In summary, we have measured the dielectron productions in $p + p$ and Au + Au collisions at 200 GeV at STAR. Within the systematic uncertainties, the dielectron production is consistent with cocktail in $p + p$ collisions.

The ω spectra are obtained in $p + p$ and minimum bias Au + Au collisions at 200 GeV. We have observed an enhancement at low mass region in minimum-bias and central Au + Au collisions. A possible modification of charm production was observed in central Au + Au collisions.

In future, two detector upgrades, Heavy Flavor Tracker (HFT) [19] and Muon Telescope Detector (MTD) [20], will help measure the charm contributions more precisely.

REFERENCES

[1] R. Rapp, J. Wambach, *Adv. Nucl. Phys.* **25**, 1 (2000).

[2] G. David, R. Rapp, Z. Xu, *Phys. Rep.* **462**, 176 (2008).

[3] H. Bichsel, *Nucl. Instrum. Methods* **A562**, 154 (2006).

[4] Y. Xu *et al.*, *Nucl. Instrum. Methods* **A614**, 28 (2010).

[5] M. Shao *et al.*, *Nucl. Instrum. Methods* **A558**, 419 (2006).

[6] J. Adams *et al.*, *Phys. Lett.* **B616**, 8 (2005).

[7] A. Adare *et al.*, *Phys. Rev.* **C81**, 034911 (2010).

[8] S.A. Voloshin *et al.*, *Z. Phys.* **C70**, 665 (1996).

[9] A.M. Poskanzer *et al.*, *Phys. Rev.* **C58**, 1671 (1998).

[10] S.A. Voloshin *et al.*, `arXiv:0809.2949v2 [nucl-ex]`.

[11] J. Adams *et al.*, *Phys. Rev. Lett.* **91**, 172302 (2003).

[12] L. Ruan *et al.*, *Nucl. Phys.* **A855**, 269 (2011).

[13] J. Zhao *et al.*, *J. Phys. G: Nucl. Part. Phys.* **38**, 124134 (2011).

[14] S.S. Adler *et al.*, *Phys. Rev.* **D83**, 052004 (2011).

[15] Z. Tang *et al.*, `arXiv:1101.1912v3 [nucl-ex]`.

[16] S.S. Adler *et al.*, *Phys. Rev.* **C75**, 051902 (2007).

[17] S.S. Adler *et al.*, *Nucl. Phys.* **A757**, 102 (2005).

[18] A. Adare *et al.*, *Phys. Rev. Lett.* **105**, 142301 (2010).

[19] S. Kleinfelder *et al.*, *Nucl. Instrum. Methods* **A565**, 132 (2006).

[20] L. Ruan *et al.*, *J. Phys. G* **36**, 095001 (2009).